Theoretical Study on the Ground State Structure of Uranofullerene U@C-82

ARTICLE *in* THE JOURNAL OF PHYSICAL CHEMISTRY A · NOVEMBER 2012

Impact Factor: 2.69 · DOI: 10.1021/jp306481e · Source: PubMed

6 AUTHORS, INCLUDING:

Xin Liu
Dalian University of Technology
62 PUBLICATIONS **717** CITATIONS
SEE PROFILE

Yuliang Zhao
Chinese Academy of Sciences
345 PUBLICATIONS **12,003** CITATIONS
SEE PROFILE

Xingfa Gao
Chinese Academy of Sciences
70 PUBLICATIONS **1,369** CITATIONS
SEE PROFILE

THE JOURNAL OF PHYSICAL CHEMISTRY A

Article

pubs.acs.org/JPCA

Theoretical Study on the Ground State Structure of Uranofullerene U@C_{82}

Xin Liu,[†] Lin Li,[†,‡] Bo Liu,[‡] Dongqi Wang,*[,§] Yuliang Zhao,[‡] and Xingfa Gao*[,‡]

[†]School of Chemistry, Dalian University of Technology, Dalian 116024, China

[‡]CAS Key Laboratory for Biomedical Effects of Nanomaterials and Nanosafety and [§]Key Laboratory of Nuclear Analysis Techniques, Institute of High Energy Physics, Chinese Academy of Sciences, Beijing 100049, China

Supporting Information

ABSTRACT: Despite its experimental characterization, the detailed geometry and electronic structure of actinide metallofullerene U@C_{82} have been rarely studied. We predict that $^{\#5}C_{82}$ and $^{\#8}C_{82}$ are the best cages for the encapsulation of monovalent and tetravalent U (i.e., U^{+} and U^{4+}), respectively; while $^{\#9}C_{82}$ is the best cage for divalent, trivalent, pentavalent, and hexavalent U cations (i.e., U^{2+}, U^{3+}, U^{5+}, and U^{6+}). U@$^{\#9}C_{82}$ is the thermodynamically most stable one among all the isomers and thus corresponds to the most experimentally isolable isomer of U@C_{82}. The calculated spin density explicitly suggests that the endohedral metallofullerene U@$^{\#9}C_{82}$ is a trivalent ion-pair with an electronic configuration of $U^{3+}@{C_{82}}^{3-}$. The proposed geometry and electronic structure of $U^{3+}@^{\#9}{C_{82}}^{3-}$ are in good agreement with the experimental observation.

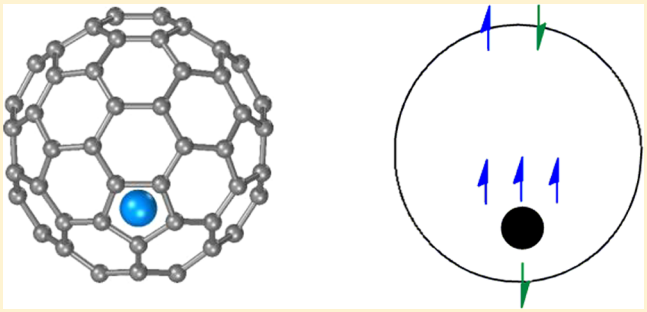

INTRODUCTION

Metals and their hybrid clusters can be encaged into fullerenes to form endohedral metallofullerenes (EMFs). The synthesis and macroscopic extraction of EMF La@C_{82} were achieved by Chai et al. in 1991.[1] Since then, EMFs have attracted broad attention for their intriguing properties attributable to the inner metals and outer cages, as well as the intramolecular metal−cage interactions. In recent years, considerable efforts have been made to synthesize new EMFs.[2−7] Most Group-2 metals, Group-3 metals, and lanthanide metals, as well as their carbide clusters and nitride clusters, have been inserted into fullerenes, and the corresponding EMFs have been isolated experimentally. Among them, the structures and chemical properties of a lot of EMFs have been explicitly characterized by experiments with the aid of calculations.

Because of the difficulties in manipulating radioactive actinides during the synthesis, the EMFs encapsulating actinide metals are rarely investigated. In 1992, Smalley and co-workers for the first time synthesized carbon−uranium clusters by vaporizing a graphite−UO_2 composite disk with laser and DC arc discharge.[8] The FT-ICR mass spectra measured for the clusters indicated the formation of various positive ions of uranium EMFs: U@C_m^{+} (m = 28, 36, 44, 58, 60, 66, 70, and 72) and U_2@C_m (m = 50, 52, 58, and 60). Photoemission spectra and calculations suggested that the C_{28} fullerene cage may have T_d symmetry and can be stabilized by accepting four electrons from uranium, forming a tetravalent ion-pair $U^{4+}@{C_{28}}^{4-}$.[8] Subsequently, Veirs and co-workers prepared uranium EMFs using a slightly different arc discharge procedure.[9] The mass spectra showed the generation of several new species with this procedure, such as U@C_{74} and U@C_{82}. The first macroscopic isolation and characterization of actinide metallofullerenes were achieved in 2001.[10] Sueki and co-workers synthesized Ac@C_{82} and Ac_2@C_{80} (Ac = U, Np, and Am) by using graphite rods containing ^{237}U, ^{239}Np, and ^{240}Am in the arc discharge and isolated the products with multistep high-performance liquid chromatography.[10] UV/vis/NIR adsorption spectra of U@C_{82} were found to have similar features as those trivalent lanthanide EMFs. In this sense, the U@C_{82} was inferred to have a trivalent electronic configuration with the form of $U^{3+}@{C_{82}}^{3-}$, which was in contrast to the tetravalent state characterized for $U^{4+}@{C_{28}}^{4-}$. However, the structural details as well as the further evidence for the trivalent electronic structure of U@C_{82} have been seldom explored.

Herein, we attempt to theoretically predict the molecular structure and associated electronic properties of U@C_{82} with respect to the experimental results of Sueki et al.[10] As the highest oxidation state of uranium is +6, we first screened out the lowest-energy fullerene structures of C_{82} carrying 0−6 negative charges, respectively (i.e., ${C_{82}}^{n-}$ with n = 0, 1, 2, 3, 4, 5, and 6). Then, we filled each of these screened structures with a uranium atom to obtain the initial geometry for U@C_{82}. After optimization of all these initial geometries, we found that uranium encaged in $^{\#8}C_{82}$ (C_{2v}) corresponds to the lowest-

Received: July 1, 2012
Revised: November 5, 2012
Published: November 7, 2012

   dx.doi.org/10.1021/jp306481e | J. Phys. Chem. A 2012, 116, 11651−11655

Table 1. Relative Energy (kcal/mol) of Ground State C_{82} and Its Anions Calculated with the B3LYP/BS1 Method[a]

C_{82} isomer[b]	C_{82}	C_{82}^{-}	C_{82}^{2-}	C_{82}^{3-}	C_{82}^{4-}	C_{82}^{5-}	C_{82}^{6-}
#1 (PA = 0)	7.8	4.6	12.6	28.8	48.7	54.7	62.0
#2 (PA = 0)	6.7	9.6	23.7	36.6	54.2	57.5	63.5
#3 (PA = 0)	0.0	1.7	14.7	23.8	36.8	41.3	47.2
#4 (PA = 0)	3.9	1.6	11.5	17.9	29.4	31.7	36.8
#5 (PA = 0)	8.3	0.0	4.2	12.3	24.6[c]	24.0	24.4
#6 (PA = 0)	12.2	0.7	2.1	3.1	9.6	10.3	14.9
#7 (PA = 0)	21.8[c]	10.6	10.0	22.5	38.8	43.7	52.0
#8 (PA = 0)	28.1[c]	12.8	9.2	2.6	0.0	4.4	12.6
#9 (PA = 0)	16.9[c]	1.5	0.0	0.0	3.8	0.0	0.0
#36458 (PA = 1)	33.4	23.8	27.3	35.6	49.0	47.9	49.6
#39662 (PA = 1)	42.8	30.9	32.9	32.7	38.9	38.7	42.2
#39663 (PA = 1)	44.0	33.0	35.3	31.9	34.4	23.6	15.1
#39704 (PA = 1)	35.4	22.4	23.6	23.9	29.9	27.4	27.7
#39686 (PA = 1)	31.0	20.3	22.1	25.4	33.8	36.5	41.7
#39656 (PA = 1)	40.8	30.9	34.9	31.7	33.7	33.4	36.1

[a]All the minima correspond to the lowest-multiplicity states unless marked otherwise. The lowest-multiplicity states for C_{82}, C_{82}^{-}, C_{82}^{2-}, C_{82}^{3-}, C_{82}^{4-}, C_{82}^{5-}, and C_{82}^{6-} are singlet, doublet, singlet, doublet, singlet, doublet, and singlet, respectively. [b]PA is the number of pentagon adjacencies. [c]These structures correspond to triplet states.

energy isomer of U@C_{82}. The calculated spin densities explicitly support that U@$^{\#9}C_{82}$ is a trivalent EMF with an electronic configuration of $U^{3+}@C_{82}^{3-}$. The predicted structure and electronic configuration are consistent with the experiment.[10]

COMPUTATIONAL METHODS

Prescreening calculations of C_{82} isomers were carried out using the BLYP[11,12] functional with 3-21G basis set[13] (BLYP/3-21G). After that, the calculations for C_{82} and C_{82}^{n-} (n = 1−6) were done with the B3LYP[11,12] functional with 6-31G(d) basis set.[14,15] For the calculations of U@C_{82} structures, the B3LYP functional in combination with 6-31G(d) basis set for C and a quasi-relativistic small-core ECP treatment (with 60 core electrons and a contraction scheme (14s13p10d8f6g)/[10s9p5d4f3g] for the valence orbital) with the corresponding valence basis set of Dolg et al.[16−18] for U (B3LYP/BS1) was used. The geometry optimizations of U@$^{\#9}C_{82}$(B) and U@$^{\#8}C_{82}$ were performed with their symmetries constrained to C_{2v} and C_s, respectively. On the basis of the optimized geometries, frequency calculations were done at the same level of theory. No imaginary frequencies were found. The geometry optimizations for U@$^{\#5}C_{82}$(A), U@$^{\#5}C_{82}$(B), and U@$^{\#9}C_{82}$(A) were carried out without symmetry constraints. All calculations were done with the Gaussian09 program.[19]

RESULTS AND DISCUSSION

Prescreening of C_{82}. We first screened a set of C_{82} fullerene cages that are probable to encapsulate U to form thermodynamically stable U@C_{82}.

Fullerenes are sp^2 carbon polyhedra consisting of 12 pentagons and a varying number of hexagons. According to Euler's polyhedron formula, the number of hexagons can be written as $N/2 - 10$, where N is the number of vertices (i.e., carbon atoms) of a fullerene. For C_{82}, it consists of 12 pentagons and 31 hexagons. These polygons may assemble in different ways, forming various topological isomers for C_{82}. Several mathematical procedures, including the spiral algorithm,[20] have been developed for the enumeration and construction of fullerene isomers.[20−22] According to the spiral algorithm, C_{82} has 9 isomers satisfying the isolated pentagon rule (IPR), i.e., each pentagon of the isomers is situated apart from other pentagons, while it also has 39 707 isomers violating the IPR rule.[20] These two kinds of isomers are usually called IPR and non-IPR fullerenes, respectively. Previous studies have established that non-IPR fullerenes are less stable than IPR fullerenes.[23] The instability of non-IPR fullerenes has been ascribed to either the local strain or π-electron destabilization pertaining to the adjacent pentagons.[20,23−28] Furthermore, theoretical studies have predicted that the thermodynamic stability of non-IPR fullerene isomers has an approximately inverse dependence with the number of pentagon adjacencies (PAs).[29−33] This suggests that C_{82} fullerenes with two or more PAs should be hard to survive in experiments, even in the form of U@C_{82}. As no non-IPR EMFs containing more PAs than the number of encapsulated metal atoms have been experimentally isolated so far and to save computational cost, we did not consider those C_{82} isomers with more than one PA in the present study. By analyzing the canonical spirals of the 39 707 non-IPR C_{82} isomers using our self-written computer code, we found 66 C_{82} with only one PA. These 66 non-IPR isomers and the 9 IPR isomers, totaling 75 C_{82} isomers, were selected for following investigation.

Lowest-Energy Isomers of C_{82} and C_{82}^{n-} (n = 1−6) Anions. We further screened the 75 C_{82} isomers obtained above in order to find the most probable cages for U@C_{82}. Previous studies show that, for the EMF isomers with the same electronic configuration $M^{n+}@C_m^{n-}$, there exists a strong correlation between their relative thermodynamic stability and that of the corresponding empty anionic cages C_m^{n-}.[34−39] In this sense, the relative stability of U@C_{82} would mainly depend on the relative stability of C_{82}^{n-}, where n is the number of electrons transferred from U to the C_{82} cage. As the highest oxidation state of uranium is +6,[40] we therefore searched the 75 prescreened C_{82} isomers for the lowest-energy C_{82}^{n-} with n = 1−6, using density functional theory calculations. Since there are still a large number of isomers (i.e., 75 × 7 = 525), we took the following steps for the calculations. We first optimized geometries for all the 75 C_{82} isomers at singlet states using the BLYP/3-21G method. On the basis of these optimized geometries, single-point (SP) energies were calculated for their trianions (C_{82}^{3-}) using the same method to evaluate the

dx.doi.org/10.1021/jp306481e | J. Phys. Chem. A 2012, 116, 11651−11655

relative stability. The calculated relative stability of neutral and trianion of these isomers is present in Table S1 of the Supporting Information. According to the relative stability order, the 15 low-lying isomers were selected for following calculations.

Table 1 shows the sequence numbers generated with the spiral algorithm[20] for the 15 selected C_{82}. As shown in Table 1, these 15 low-lying isomers include all the nine IPR C_{82} ($^{\#1}C_{82}$ through $^{\#9}C_{82}$) and six non-IPR C_{82} ($^{\#36458}C_{82}$, $^{\#39662}C_{82}$, $^{\#39663}C_{82}$, $^{\#39704}C_{82}$, $^{\#39686}C_{82}$, and $^{\#39656}C_{82}$). The geometries of each isomer and the corresponding C_{82}^{n-} anions (n = 1−6) were reoptimized at B3LYP/6-31G(d) level. The optimizations for the neutral and C_{82}^{n-} with n = 2, 4, and 6 were performed for singlet and triplet states to locate the ground states, while the calculations for C_{82}^{n-} with n = 1, 3, and 5 were performed for doublet and quartet states. As shown in Table 1, the lowest-energy isomer for neutral C_{82} is singlet $^{\#3}C_{82}$, which is in good agreement with the previous studies.[41−52] The stability order of the other neutral C_{82} is also consistent with that predicted by the previous work.[52] The lowest-energy isomers for C_{82}^{n-} with n = 1−6 are doublet $^{\#5}C_{82}$, singlet $^{\#9}C_{82}$, doublet $^{\#9}C_{82}$, singlet $^{\#8}C_{82}$, doublet $^{\#9}C_{82}$, and singlet $^{\#9}C_{82}$, respectively. Therefore, $^{\#5}C_{82}$ and $^{\#8}C_{82}$ are, respectively, the best cages for the encapsulation of monovalent and tetravalent U (i.e., U^{+} and U^{4+}), while $^{\#9}C_{82}$ is the best cage for divalent, trivalent, pentavalent, and hexavalent U (i.e., U^{2+}, U^{3+}, U^{5+}, and U^{6+}). The relative stabilities of U@$^{\#5}C_{82}$, U@$^{\#8}C_{82}$, and U@$^{\#9}C_{82}$ were also thus studied to find the lowest-energy isomer for U@C_{82} (see below).

Lowest-Energy Isomer of U@C_{82}. We placed U atoms into $^{\#9}C_{82}$, $^{\#5}C_{82}$, and $^{\#8}C_{82}$ cages to study their relative stability by DFT calculations. Isomers $^{\#5}C_{82}$ and $^{\#9}C_{82}$ are of C_2 point group symmetry. For each of these C_2 isomers, we put U atom at two different positions inside the cage to set up two different initial geometries, i.e., the off-center positions along the C_2 axis close to the two ends of the axis. So these U@C_{82} isomers also have the C_2 symmetry. For $^{\#8}C_{82}$ of C_s symmetry, we put U at two opposite off-center positions on the mirror plane to set up the two initial geometries with C_s symmetry. Geometry optimizations were performed for these U@C_{82} isomers at triplet states using the B3LYP/BS1 method. The reason for first doing calculations for triplet states was that most lanthanide EMFs Ln@C_{82}, including Nd@C_{82}, have triplet ground states.

The calculations of five isomers converged, whose structures are displayed in Figure 1 as U@$^{\#9}C_{82}$ (A), U@$^{\#9}C_{82}$ (B), U@$^{\#5}C_{82}$ (A), U@$^{\#5}C_{82}$ (B), and U@$^{\#8}C_{82}$. The relative stability of these isomers is listed in Table 2. Among the five triplet isomers, U@$^{\#9}C_{82}$ (B) has the lowest energy. U@$^{\#9}C_{82}$ (B) corresponds to the encapsulation of the U atom at the position B of $^{\#9}C_{82}$. Position B is along the C_2 axis near the hexagonal ring of $^{\#9}C_{82}$, which is shown in a yellow color in Figure 1. Moving U atom to the opposite position A, i.e., the position near the C−C bond of $^{\#9}C_{82}$ (also shown in yellow) forms U@$^{\#9}C_{82}$ (A). However, U@$^{\#9}C_{82}$ (A) is less stable than U@$^{\#9}C_{82}$ (B) by 34.0 kcal/mol. The second lowest-energy triplet isomer is U@$^{\#8}C_{82}$, which is less stable than U@$^{\#9}C_{82}$ (B) by only 5.6 kcal/mol (Figure 1 and Table 2). U@$^{\#5}C_{82}$ (A) and U@$^{\#5}C_{82}$ (B) correspond to $^{\#5}C_{82}$ encapsulating U atom at positions near the C−C bond and hexagonal ring of $^{\#5}C_{82}$ cage, respectively (the C−C bond and hexagonal ring are shown in a yellow color; see Figure 1). They have energies higher than U@$^{\#9}C_{82}$ (B) by 64.4 and 16.2 kcal/mol, respectively. Similar to the case of U@$^{\#9}C_{82}$, U@$^{\#5}C_{82}$(B) with U near the hexagon is more stable than U@$^{\#5}C_{82}$(A) with U near the C−C bond. The preference of U atom to the hexagonal ring over the C−C bond is consistent with the previous findings,[53−55] which might be ascribed to that U near the hexagonal ring has a larger number of coordination with the C_{82} cage than U near the double bond does so gains a large stabilization effect.

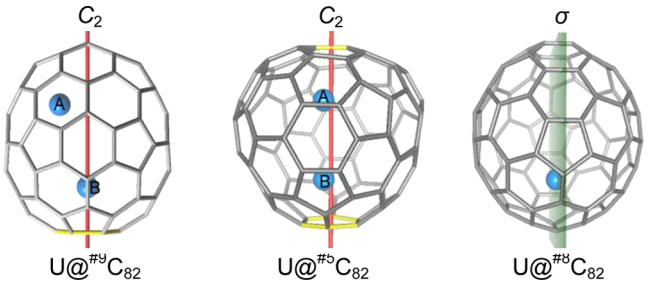

Figure 1. Schematic structures of U@C_{82} isomers: U@$^{\#9}C_{82}$(A), U@$^{\#9}C_{82}$(B), U@$^{\#5}C_{82}$(A), U@$^{\#5}C_{82}$(B), and U@$^{\#8}C_{82}$. The C_2 axes (C_2) of $^{\#9}C_{82}$ and $^{\#5}C_{82}$ and the symmetry plane (σ) of $^{\#8}C_{82}$ are shown. A and B in U@$^{\#9}C_{82}$ and U@$^{\#5}C_{82}$ label the positions of U with respect to the C_2 axis of the pristine C_{82} cages.

Table 2. Relative Energy (E_{rel}, kcal/mol), $\langle S^2\rangle$, and Spin Densities Located on U and C_{82} Cage (S_U and S_{cage})[a] of U@C_{82} Isomers Calculated at Different States

isomer	state	E_{rel}[b]	$\langle S^2\rangle$[b]	S_U[b]	S_{cage}[b]
U@$^{\#9}C_{82}$(A)	triplet	34.0	3.06	+3.0	−1.0
U@$^{\#9}C_{82}$(B)	triplet	0.0	2.91	+3.0	−1.0
U@$^{\#5}C_{82}$(A)	triplet	64.6	3.02	+3.1	−1.1
U@$^{\#5}C_{82}$(B)	triplet	16.2	3.01	+3.1	−1.1
U@$^{\#8}C_{82}$	triplet	5.6	2.85	+3.0	−1.0
U@$^{\#9}C_{82}$(A)	CS	36.4		0	0
U@$^{\#9}C_{82}$(A)	OS	30.7	0.87	+1.0	−1.0
U@$^{\#9}C_{82}$(A)	quintet	2.4	6.02	+3.1	+0.9

[a] S_U and S_{cage} represent the sums of Mulliken spins on the U atom and the C_{82} cage, respectively. The plus and minus signs represent the up and down orientations of the spins, respectively. [b] Calculated with the B3LYP/BS1 method.

Ground-State Electronic Configuration of U@C_{82}. To confirm the ground state geometry and electronic structure, the geometry of U@$^{\#9}C_{82}$(A) was reoptimized in closed-shell singlet (CS), open-shell singlet (OS), and quintet. As shown in Table 2, CS, OS, and quintet U@$^{\#9}C_{82}$(A) have energy higher than the triplet by 36.4, 30.7, and 2.4 kcal/mol, respectively. These results confirmed that the ground state of U@$^{\#9}C_{82}$ should be triplet. The quintet state is found less stable than the triplet by 2.4 kcal/mol.

According to Table 1, $^{\#9}C_{82}$ is suitable for encaging divalent, trivalent, pentavalent, and hexavalent U cations. To determine the most probable electronic configuration for U@C_{82}, we analyzed the spin density distributions for U@$^{\#9}C_{82}$(A) at ground and excited states.

Figure 2a shows the spin density distributions of the OS, triplet, and quintet of U@$^{\#9}C_{82}$(A) calculated using the B3LYP/BS1 method. As shown in Figure 2a, the spin densities on U/C_{82} (denoted as S_U/S_{cage}, see Figure 2) of the OS, triplet, and quintet are +1.0/−1.0, +3.0/−1.0, and +3.1/+0.9, respectively. The plus and minus signs represent up and down spin orientations, respectively. On the basis of these

dx.doi.org/10.1021/jp306481e | J. Phys. Chem. A 2012, 116, 11651−11655

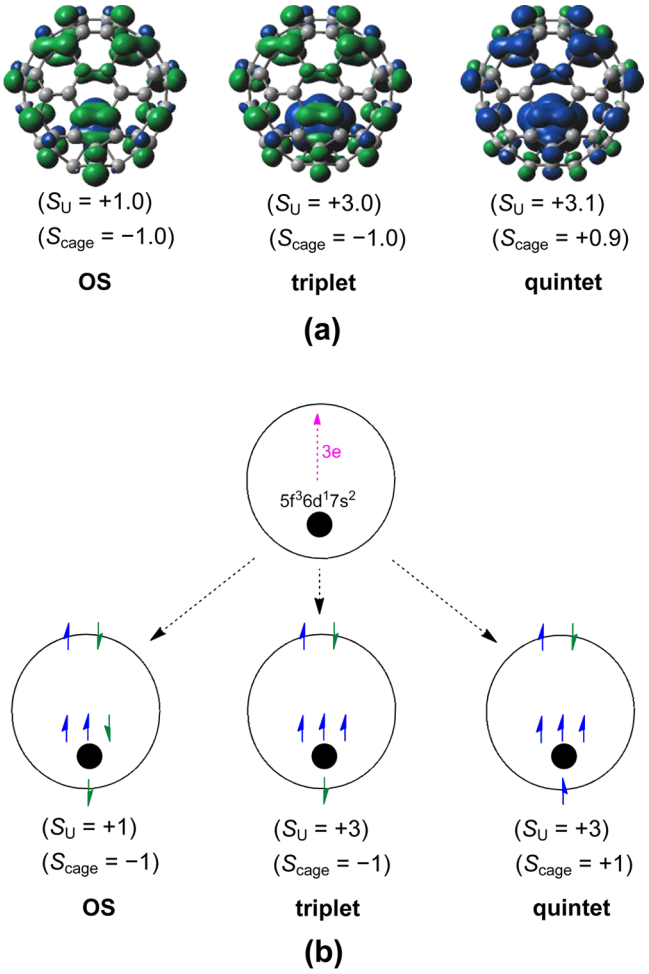

Figure 2. Electronic structure of U@$^{\#9}C_{82}$(A): (a) spin density distribution calculated for the open-shell singlet (OS), triplet, and quintet states with the B3LYP/BS1 method; (b) cartoon illustration for the electron transfer from U to C_{82} cage and the singlet, triplet, and quintet arrangements of the valence electrons on U and C_{82}. In panels a and b, S_U and S_{cage} represent the sums of spins on the U atom and the C_{82} cages, respectively, with plus and minus signs representing the up and down alignments of the spins, respectively. These S_U and S_{cage} values of (a) were obtained from the DFT calculation and can also be found in Table 2. In panels a and b, the up and down spins are differentiated with blue and green colors, respectively.

results, the following electronic configuration can be predicted for U@$^{\#9}C_{82}$(A): U atom, which has a valence electronic configuration of $5f^3 6d^1 7s^2$, transfers three electrons to the $^{\#9}C_{82}$ cage (Figure 2b, top panel), leading to an electronic configuration with three electrons in the 5f orbitals of U ($5f^3$) and other three electrons on the $^{\#9}C_{82}$ cage. The three 5f electrons of U and three cage electrons can adopt different spin arrangements to produce the singlet, triplet, and quintet states, as shown in Figure 2b. The three electrons on the C_{82} cage always take a low-spin configuration with a spin density of one (S_{cage} = −1 for OS and triplet, and S_{cage} = +1 for quintet; see Figure 2b). However, the 5f electrons of U may either take a low-spin configuration to maintain a spin density of one for U in the OS (S_U = +1) or take a high-spin configuration to generate a spin density of three for U in the triplet and quintet (S_U = +3). The triplet and quintet correspond to the cage's net spin electrons taking an antiferromagnetic and ferromagnetic coupling with the U's net spin electrons, respectively. One can see that the S_U and S_{cage} values predicted with the electronic configurations of Figure 2b are in excellent agreement with those of Figure 2a, which were obtained from DFT calculations. Except for the trivalent configuration (i.e., transferring three electrons from U to C_{82}), none of the divalent, pentavalent, and hexavalent configurations can explain the DFT-calculated spin density distributions, i.e., S_U/S_{cage} of Figure 2a. Suppose U transfers two electrons to C_{82} to form the divalent configuration, then the S_U/S_{cage} for the OS should take a value of 0/0 or 2/2; the S_U/S_{cage} for the triplet should take a value of 0/2 or 2/0; the S_U/S_{cage} for the quintet should take a value of 4/0 or 2/2. Suppose U transfers five (six) electrons to C_{82} to form the pentavalent (hexavalent) configuration, then the S_U at any state should take the value of 1 (0). All these values do not match the corresponding S_U/S_{cage} calculated by DFT. This suggests that the DFT results exclusively support the trivalent electronic configuration for U@$^{\#9}C_{82}$ (i.e., U^{3+}@$^{\#9}C_{82}^{3-}$). The predicted structure and electronic structure of U^{3+}@$^{\#9}C_{82}^{3-}$ profoundly explain the similarity between the UV/vis/NIR adsorption spectra measured for U@C_{82} and those for lanthanide EMFs, which were characterized as Ln^{3+}@$^{\#9}C_{82}^{3-}$.[10] It should be noted that, although the B3LYP method predicts the triplet ground state for U@C_{82} that is consistent with the experimental observations, the B3LYP method failed to predict the experimentally suggested ground state for Gd@C_{82}.[56] Therefore, caution should be taken when using this method in the related studies in the future.

Table 2 also gives the DFT spins for U@$^{\#5}C_{82}$ and U@$^{\#8}C_{82}$. Similar analysis suggests that U@$^{\#5}C_{82}$ and U@$^{\#8}C_{82}$ exhibit a trivalent configuration as U@$^{\#9}C_{82}$, although their cages are the most suitable C_{82} cages for the encapsulation of monovalent and tetralent cations, respectively.

CONCLUSIONS

C_{82} fullerene has nine IPR-isomers, 66 non-IPR isomers with one PA, and 39 641 non-IPR isomers with two or more PAs. Because of the instability associated with PA, C_{82} isomers with over one PA are less possible to be stabilized by encapsulating a single U atom and to survive in the experimental isolation. According to the DFT results, $^{\#5}C_{82}$ and $^{\#8}C_{82}$ are the best cages for the encapsulation of monovalent and tetravalent U (i.e., U^+ and U^{4+}), respectively; while $^{\#9}C_{82}$ is the best cage for divalent, trivalent, pentavalent, and hexavalent U (i.e., U^{2+}, U^{3+}, U^{5+}, and U^{6+}). U@$^{\#9}C_{82}$ corresponds to the thermodynamically most stable (experimentally viable) isomer of U@C_{82}, where U stands adjacent to the hexagonal ring along the C_2 axis of the C_{82}. U@$^{\#9}C_{82}$ is a triplet at ground state, with an antiferromagnetic coupling between the spins of the cage and the U metal. The calculated spin densities for U@$^{\#9}C_{82}$'s triplet, OS, and quintet exclusively support that U@$^{\#9}C_{82}$ is a trivalent EMF with an electronic configuration of U^{3+}@C_{82}^{3-}. The predicted structure and electronic structure of U^{3+}@$^{\#9}C_{82}^{3-}$ are in good agreement with the experimental observations. Therefore, the calculation scheme used here can also be applied to study the structures and electronic structures for other actinide metallofullerenes in the future.

ASSOCIATED CONTENT

Supporting Information

Energy for neutral C_{82} and C_{82}^{3-}. This material is available free of charge via the Internet at http://pubs.acs.org.

dx.doi.org/10.1021/jp306481e | J. Phys. Chem. A 2012, 116, 11651−11655

AUTHOR INFORMATION

Corresponding Author

*E-mail: dwang@ihep.ac.cn (D.W.); gaox@ihep.ac.cn (X.G.).

Notes

The authors declare no competing financial interest.

ACKNOWLEDGMENTS

This work was supported by MOST 973 program of China (2012CB934001, 2012CB932504, and 2011CB933403) and CAS Hundreds Elite Program (Y1515530U1 and Y1515540U1). X.L. thanks NSFC (21103015, 20273012, and 11174045), the Chinese Scholarship Council (2009606533), the Fundamental Research Funds for the Central Universities (DUT11LK19 and DUT12LK14), and the Key Laboratory of Coastal Zone Environmental Processes YICCAS (201203) for financial support. We thank Dr. Jingyan Shi and Dr. Bowen Kan of IHEP for assistance concerning the use of computer equipment.

REFERENCES

(1) Chai, Y.; Guo, T.; Jin, C.; Haufler, R. E.; Chibante, L. P. F.; Fure, J.; Wang, L.; Alford, J. M.; Smalley, R. E. *J. Phys. Chem.* **1991**, *95*, 7564−7568.

(2) Shinohara, H. *Rep. Prog. Phys.* **2000**, *63*, 843−892.

(3) Rodríguez-Fortea, A.; Balch, A. L.; Poblet, J. M. *Chem. Soc. Rev.* **2011**, *40*, 3551−3563.

(4) Yamada, M.; Akasaka, T.; Nagase, S. *Acc. Chem. Res.* **2010**, *43*, 92−102.

(5) Tan, Y.-Z.; Xie, S.-Y.; Huang, R.-B.; Zheng, L.-S. *Nat. Chem.* **2009**, *1*, 450−458.

(6) Dunsch, L.; Yang, S. *Small* **2007**, *3*, 1298−1320.

(7) Chaur, M. N.; Melin, F.; Ortiz, A. L.; Echegoyen, L. *Angew. Chem., Int. Ed.* **2009**, *48*, 7514−7538.

(8) Guo, T.; Diener, M. D.; Chai, Y.; Alford, M. J.; Haufler, R. E.; McClure, S. M.; Ohno, T.; Weaver, J. H.; Scuseria, G. E.; Smalley, R. E. *Science* **1992**, *257*, 1661−1664.

(9) Diener, M. D.; Smith, C. A.; Veirs, D. K. *Chem. Mater.* **1997**, *9*, 1773−1777.

(10) Akiyama, K.; Zhao, Y.; Sueki, K.; Tsukada, K.; Haba, H.; Nagame, Y.; Kodama, T.; Suzuki, S.; Ohtsuki, T.; Sakaguchi, M.; et al. *J. Am. Chem. Soc.* **2001**, *123*, 181−182.

(11) Becke, A. D. *Phys. Rev. A* **1988**, *38*, 3098−3100.

(12) Lee, C.; Yang, W.; Parr, R. G. *Phys. Rev. B* **1988**, *37*, 785−789.

(13) Binkley, J. S.; Pople, J. A.; Hehre, W. J. *J. Am. Chem. Soc.* **1980**, *102*, 939−947.

(14) Hehre, W. J.; Ditchfield, R.; Pople, J. A. *J. Chem. Phys.* **1972**, *56*, 2257−2261.

(15) Hariharan, P. C.; Pople, J. A. *Mol. Phys.* **1974**, *27*, 209−214.

(16) Kuchle, W.; Dolg, M.; Stoll, H.; Preuss, H. *J. Chem. Phys.* **1994**, *100*, 7535−7542.

(17) Cao, X. Y.; Dolg, M.; Stoll, H. *J. Chem. Phys.* **2003**, *118*, 487−496.

(18) Cao, X.; Dolg, M. *J. Molec. Struct.* **2004**, *673*, 203−209.

(19) Frisch, M. J.; Trucks, G. W.; Schlegel, H. B.; Scuseria, G. E.; Robb, M. A.; Cheeseman, J. R.; Scalmani, G.; Barone, V.; Mennucci, B.; Petersson, G. A.; et al.; *Gaussian 09*, revision A01; Gaussian, Inc., Wallingford CT, 2009.

(20) Fowler, P. W.; Manolopoulos, D. E. *An Altlas of Fullerenes*; Clarendon Press: Oxford, U.K., 1995.

(21) Ōsawa, E.; Ueno, H.; Yoshida, M.; Slanina, Z.; Zhao, X.; Nishiyama, M.; Saito, H. *J. Chem. Soc., Perkin Trans. 2* **1998**, *2*, 943−950.

(22) Brinkmann, G.; Friedrichs, O. D.; Lisken, S.; Peeters, A.; Cleemput, N. V. *MATCH Commun. Math. Comput. Chem.* **2010**, *63*, 533−552.

(23) Kroto, H. W. *Nature* **1987**, *329*, 529−531.

(24) Schmalz, T. G.; Seitz, W. A.; Klein, D. J.; Hite, G. E. *Chem. Phys. Lett.* **1986**, *130*, 203−207.

(25) Schmalz, T. G.; Seitz, W. A.; Klein, D. J.; Hite, G. E. *J. Am. Chem. Soc.* **1988**, *110*, 1113−1127.

(26) Aihara, J.-I. *J. Am. Chem. Soc.* **1995**, *117*, 4130−4136.

(27) Haddon, R. C. *Science* **1993**, *17*, 1545−1550.

(28) Kovalenko, V. I.; Khamatgalimov, A. R. *Russ. Chem. Rev.* **2006**, *75*, 981−988.

(29) Campbell, E. E. B.; Fowler, P. W.; Mitchell, D.; Zerbetto, F. *Chem. Phys. Lett.* **1996**, *250*, 544−548.

(30) Rodríguez-Fortea, A.; Alegret, N.; Balch, A. L.; Poblet, J. M. *Nat. Chem.* **2010**, *2*, 955−961.

(31) Gao, X.; Zhao, Y. *J. Comput. Chem.* **2007**, *28*, 795−801.

(32) Achiba, Y.; Fowler, P. W.; Mitchell, D.; Zerbetto, F. *J. Phys. Chem. A* **1998**, *102*, 6835−6841.

(33) Austin, S. J.; Fowler, P. W.; Manolopoulos, D. E.; Orlandi, G.; Zerbetto, F. *J. Phys. Chem.* **1995**, *99*, 8076−8081.

(34) Kobayashi, K.; Nagase, S. *Chem. Phys. Lett.* **1997**, *274*, 226−230.

(35) Campanera, J. M.; Bo, C.; Poblet, J. M. *Angew. Chem., Int. Ed.* **2005**, *44*, 7230−7233.

(36) Popov, A. A.; Dunsch, L. *J. Am. Chem. Soc.* **2007**, *129*, 11835−11849.

(37) Chaur, M. N.; Valencia, R.; Rodríguez-Fortea, A.; Poblet, J. M.; Echegoyen, L. *Angew. Chem., Int. Ed.* **2009**, *48*, 1425−1428.

(38) Yang, S.; Popov, A. A.; Dunsch, L. *Angew. Chem., Int. Ed.* **2007**, *46*, 1256−1259.

(39) Zheng, J.; Zhao, X.; Dang, J.; Chen, Y.; Xu, Q.; Wang, W. *Chem. Phys. Lett.* **2011**, *514*, 104−108.

(40) Wang, D.; van Gunsteren, W. F.; Chai, Z. *Chem. Soc. Rev.* **2012**, *41*, 5836−5865.

(41) Kobayashi, K.; Nagase, S. *Chem. Phys. Lett.* **1998**, *282*, 325−329.

(42) Orlandi, G.; Zerbetto, F.; Fowler, P. W. *J. Phys. Chem.* **1993**, *97*, 13575−13579.

(43) Wang, X. Q.; Wang, C. Z.; Zhang, B. L.; Ho, K. M. *Chem. Phys. Lett.* **1994**, *217*, 199−203.

(44) Slanina, Z.; Lee, S.-L.; Kobayashi, K.; Nagase, S. *J. Mol. Struct.* **1995**, *339*, 89−93.

(45) Nagase, S.; Kobayashi, K.; Akasaka, T. *Bull. Chem. Soc. Jpn.* **1996**, *69*, 2131−2142.

(46) Seifert, G.; Bartl, A.; Dunsch, L.; Ayuela, A.; Rockenbauer, A. *Appl. Phys. A: Mater. Sci. Process* **1998**, *66*, 265−271.

(47) Cioslowski, J.; Rao, N.; Moncrieff, D. *J. Am. Chem. Soc.* **2000**, *122*, 8265−8270.

(48) Chen, Z.; Cioslowski, J.; Rao, N.; Moncrieff, D.; Bühl, M.; Hirsch, A.; Thiel, W. *Theor. Chem. Acc.* **2001**, *106*, 364−368.

(49) Sun, G.; Kertesz, M. *J. Phys. Chem. A* **2001**, *105*, 5468−5472.

(50) Zheng, G.; Irle, S.; Morokuma, K. *Chem. Phys. Lett.* **2005**, *412*, 210−216.

(51) Zalibera, M.; Popov, A. A.; Kalbac, M.; Rapta, P.; Dunsch, L. *Chem.—Eur. J.* **2008**, *14*, 9960−9967.

(52) Khamatgalimov, A. R.; Kovalenko, V. I. *J. Phys. Chem. A* **2011**, *115*, 12315−12320.

(53) Lu, X.; Lian, Y.; Beavers, C. M.; Mizorogi, N.; Slanina, Z.; Nagase, S.; Akasaka, T. *J. Am. Chem. Soc.* **2011**, *133*, 10772−10775.

(54) Mizorogi, N.; Nagase, S. *Chem. Phys. Lett.* **2006**, *431*, 110−112.

(55) Liu, L.; Gao, B.; Chu, W.; Chen, D.; Hu, T.; Wang, C.; Dunsch, L.; Marcelli, A.; Luo, Y.; Wu, Z. *Chem. Commun.* **2008**, 474−476.

(56) Sebetci, A.; Richter, M. *J. Phys. Chem. C* **2010**, *114*, 15−19.

NOTE ADDED IN PROOF

For more computational studies on uranofullerene, see: Infante, I.; Gagliardi, L.; Scuseria, G. E. *J. Am. Chem. Soc.* **2008**, *130*, 7459−7465; Wu, X.; Lu, X. *J. Am. Chem. Soc.* **2007**, *129*, 2171−2177.